

AD722060

AFML-TR-71-53

**RESEARCH AND DEVELOPMENT OF  
RARE EARTH-TRANSITION METAL ALLOYS  
AS PERMANENT-MAGNET MATERIALS**

**A. E. Ray and K. J. Strnat  
Research Institute  
University of Dayton**

**Sponsored by  
Advanced Research Projects Agency  
ARPA Order No. 1617**

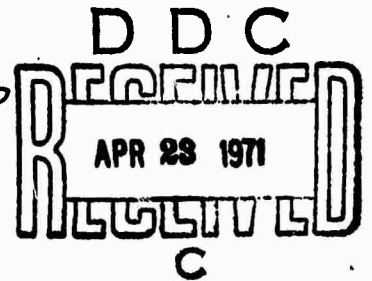
**TECHNICAL REPORT AFML-TR-71-53  
March 1971**

**DISTRIBUTION STATEMENT A**

Approved for public release;  
Distribution Unlimited

Distribution of this document is unlimited.

**Air Force Materials Laboratory  
Wright-Patterson Air Force Base  
Air Force Systems Command  
Dayton, Ohio**



The views and conclusions contained in this document are those of the authors and should not be interpreted as necessarily representing the official policies, either expressed or implied, of the Advanced Research Projects Agency or the U.S. Government.

Reproduced by  
**NATIONAL TECHNICAL  
INFORMATION SERVICE**  
Springfield, Va. 22151

NOTICE

When Government drawings, specifications, or other data are used for any purpose other than in connection with a definitely related Government procurement operation, the United States Government thereby incurs no responsibility nor any obligation whatsoever; and the fact that the Government may have formulated, furnished, or in any way supplied the said drawings, specifications, or other data, is not to be regarded by implication or otherwise as in any manner licensing the holder or any other person or corporation, or conveying any rights or permission to manufacture, use, or sell any patented invention that may in any way be related thereto.

ACCESSION NO.		
GPST	WHITE SECTION	<input checked="" type="checkbox"/>
DDG	BUFF SECTION	<input type="checkbox"/>
UNANNOUNCED		<input type="checkbox"/>
JUSTIFICATION		
BY		
DISTRIBUTION/AVAILABILITY CODES		
DISC.	AVAIL.	ADD/ or SPECIAL
A		

Copies of this report should not be returned unless return is required by security considerations, contractual obligations, or notice on a specific document.

RESEARCH AND DEVELOPMENT OF RARE EARTH-TRANSITION  
METAL ALLOYS AS PERMANENT-MAGNET MATERIALS

By:

Dr. Alden E. Ray and Dr. Karl J. Strnat, Principal Investigators  
University of Dayton, Research Institute and Electrical Engineering Dept.  
300 College Park Ave., Dayton, Ohio 45409  
Tel. Numbers: (513) 229-3527 and (513) 229-3611

Sponsored by  
Advanced Research Projects Agency  
ARPA Order No. 1617

**Details of illustrations in  
this document may be better  
studied on microfiche**

Program Code No. OD10  
Contract effective date: 30 June 1970  
Expiration date: 30 June 1973  
Amount of contract: \$525,012

Submitted to:

Air Force Materials Laboratory, AFSC, USAF  
Project Engineer: Capt. M. V. Turner, LPE Tel. (513) 255-4474

Distribution of this document is unlimited.

This research was supported by the Advanced Research Projects Agency of the Department of Defense and was monitored by the Air Force Materials Laboratory, AFSC, USAF under Contract No. F33615-70-C-1625.

## FOREWORD

The research described in this report is part of the contractual research program of the Materials Physics Division, Air Force Materials Laboratory. It was performed by the authors at the University of Dayton, Research Institute and was sponsored by the Advanced Research Projects Agency, ARPA Order No. 1617, Program Code No. OD10. The contract is administered under Project No. 7371, Task No. 737103, by the Air Force Materials Laboratory, Research and Technology Division, Air Force Systems Command, Wright-Patterson Air Force Base, Ohio.

This report covers research conducted between 30 June 1970 and 31 December 1970. The manuscript was released by the authors in February 1971 for publication as a technical report.

This technical report has been reviewed and is approved.

  
CHARLES E. EHRENFRIED,

Major, USAF

Chief, Electromagnetic  
Materials Branch

Materials Physics Division

Air Force Materials Laboratory

## ABSTRACT

Intermetallic phases with the formulas  $R_2Co_{17}$ ,  $R_2Fe_{17}$ , and  $R_2(Co_{1-x}Fe_x)_{17}$  are of potential interest as permanent magnets. Procedures for the preparation of these intermetallic phases are described. Descriptions are given of the design and operation of differential thermal analysis equipment and of a high temperature-high vacuum furnace for the metallurgical and magnetic evaluation of rare earth-transition metal intermetallic phases.

## TABLE OF CONTENTS

<u>Section</u>	<u>Page</u>
I	INTRODUCTION..... 1
1.	THE PHASE DIAGRAMS OF THE RARE EARTHS WITH IRON AND WITH COBALT..... 3
2.	CRUCIBLE MATERIALS..... 3
3.	RARE EARTH METALS..... 5
4.	MELTING PROCEDURES FOR RARE EARTH-TRANSITION METAL ALLOYS..... 8
5.	PROCEDURES FOR THE PREPARATION OF SINGLE PHASE ALLOYS OF $R_2Co_{17}$ , $R_2Fe_{17}$ , AND $R_2(Co_{1-x}Fe_x)_{17}$ ..... 11
a.	$R_2Co_{17}$ Phases..... 11
b.	$R_2Fe_{17}$ Phases..... 16
c.	$R_2(Co_{1-x}Fe_x)_{17}$ Phases..... 18
II	DIFFERENTIAL THERMAL ANALYSIS APPARATUS..... 21
1.	INTRODUCTION..... 21
2.	COMPONENTS..... 22
a.	Thin Film Evaporator..... 22
b.	DTA Module..... 22
c.	Solid State Temperature Controller..... 25
d.	Programmer..... 26
e.	Saturable Core Reactor..... 26
f.	Transformers..... 26
g.	X-Y Recorder..... 27
h.	Inert Gas Purification Train..... 27
III	DIFFERENTIAL THERMAL ANALYSIS OF SOME $R_2Co_{17}$ PHASES..... 30
IV	DESIGN AND CONSTRUCTION OF A HIGH TEMPERATURE-HIGH VACUUM TUBULAR FURNACE..... 32
1.	INTRODUCTION..... 32
2.	GENERAL DESCRIPTION..... 32

<u>Section</u>	<u>Page</u>
a. Furnace.....	32
b. Electrical Temperature Control System.....	35
c. Vacuum System.....	36
d. Furnace Drive System.....	37
3. OPERATIONAL PERFORMANCE.....	39
REFERENCES.....	41

## LIST OF ILLUSTRATIONS

<u>Figure</u>	<u>Page</u>
1. Phase diagrams for six rare earth-cobalt alloy systems.....	4
2. Interface between a Pr-86 at. %Fe alloy and $\text{Al}_2\text{O}_3$ heated to $1450^\circ\text{C}$ . 75 X.....	6
3. Interface between a Pr-86 at. %Fe alloy and $\text{MgO}$ heated to $1450^\circ\text{C}$ . 75 X.....	6
4. Interface between a Pr-86 at. %Fe alloy and $\text{ZrO}_2$ heated to $1450^\circ\text{C}$ . 75 X.....	6
5. Interface between a Pr-86 at. %Fe alloy and tantalum (Ta) heated to $1450^\circ\text{C}$ . .....	7
6. Interface between a Pr-86 at. %Fe alloy and $\text{Y}_2\text{O}_3$ heated to $1450^\circ\text{C}$ . 75 X.....	7
7. Arc melted Ce-89.5 at. %Co alloy. Cobalt dendrites peritectically surrounded by $\text{Ce}_2\text{Co}_{17}$ . The dark phase is $\text{CeCo}_5$ . 250 X.....	13
8. Arc melted Pr-89 at. % Co alloy. This alloy is primarily $\text{Pr}_2\text{Co}_{17}$ with some $\text{PrCo}_5$ and just detectable amounts of free cobalt. 250 X.....	13
9. Arc melted Nd-89 at. %Co alloy. This alloy is essentially single phase $\text{Nd}_2\text{Co}_{17}$ even though $\text{Nd}_2\text{Co}_{17}$ forms by peritectic reaction. 250 X.....	13
10. Ce-89.5 at. %Co homogenized 32 hours at $1100^\circ\text{C}$ . $\text{Ce}_2\text{Co}_{17}$ with excess cobalt as dendrites. 250 X.....	14
11. Ce-89 at. %Co homogenized 50 hours at $1100^\circ\text{C}$ . $\text{Ce}_2\text{Co}_{17}$ with excess cerium as $\text{CeCo}_5$ . 250 X.....	14
12. Pr-89 at. %Co homogenized 50 hours at $1100^\circ\text{C}$ . Single phase $\text{Pr}_2\text{Co}_{17}$ , light and dark regions are annealing twins. 250 X.....	15
13. Nd-89 at. %Co homogenized 50 hours at $1100^\circ\text{C}$ . Single phase $\text{Nd}_2\text{Co}_{17}$ . 250 X.....	15



<u>Figure</u>	<u>Page</u>
14. Y-89 at. %Co homogenized 50 hours at 1100°C. $Y_2Co_{17}$ plus an unidentified phase segregated to the grain boundaries. It is suspected this second phase material was carried over from the yttrium used for alloying. 250 X.....	15
15. Arc melted Ce-89 at. %Fe showing gross segregation which develops on solidification. The average composition of the bottom portion (thick dendrites) is about 95 at. %Fe, the top portion about 87.5 at. %Fe. 50 X.....	17
16. Ce-89 at. %Fe homogenized 8 hours at 875°C, showing how the gross segregation developed on solidification (Figure 15) persists after homogenization. The top portion of alloy is essentially single phase $Ce_2Fe_{17}$ while the bottom portion is iron in a matrix of $Ce_2Fe_{17}$ . 50 X.....	17
17. Pr-87 at. %Fe homogenized 8 hours at 1000°C. Large grains of $Pr_2Fe_{17}$ , some heavily twinned, with dark voids which originally contained Pr + $Pr_2Fe_{17}$ eutectic. 250 X.....	19
18. $MM_2(Co_{.75}Fe_{.25})_{17}$ alloy homogenized 50 hours at 1100°C. 250 X.....	19
19. DTA - Module.....	24
20. DTA circuits and components.....	28
21. Inert gas purification.....	29
22. Overall view of high temperature-high vacuum furnace system....	33
23. Block diagram, high temperature-high vacuum furnace system....	34
24. Drive system for furnace carriage, showing lead screw with coupling link to furnace (above), motor with speed reducer and electronic speed controller.....	38

## SECTION I

### INTRODUCTION

The binary cobalt-rich and iron-rich intermetallic phases which exist in rare earth alloy systems are compared in Table I. The number and types of intermetallic phases are quite different. However, for each  $R_2Co_{17}$  phase, there is a corresponding  $R_2Fe_{17}$  phase isostructural to it. All of the  $R_2Co_{17}$  phases have higher Curie temperatures and higher saturation magnetizations than their  $RCo_5$  counterparts. Unfortunately, most of the  $R_2Co_{17}$  phases have the wrong kind of magnetocrystalline anisotropy, i. e., an easy basal plane and a hard c-axis.  $Sm_2Co_{17}$  was found to have an easy axis but an anisotropy constant only about half that of  $SmCo_5$ . The  $R_2Fe_{17}$  have much higher saturation magnetizations than even the  $R_2Co_{17}$  phases. However, the Curie temperatures of these phases are too low to make them of interest, as such, for most permanent-magnet applications. Little is known, at present, concerning the magnetocrystalline anisotropy of the  $R_2Fe_{17}$  phases. We are investigating the alloying behavior of the  $R_2Co_{17}$  and  $R_2Fe_{17}$  phases to see if a useful balance can be attained between the high Curie temperatures of the  $R_2Co_{17}$  phases and the high saturation magnetizations of the  $R_2Fe_{17}$  phases. Such alloying combinations are likely to strongly influence the magnetocrystalline anisotropies of the components, and may well be the effect needed to induce a favorable magnetic symmetry in these alloys.

Most of our efforts to date have been directed at developing techniques for preparing the alloys and procedures for evaluating them. In this Section, the procedures for preparing  $R_2Co_{17}$ ,  $R_2Fe_{17}$ , and  $R_2(Co_{1-x}Fe_x)_{17}$  alloys are described. We have concentrated our efforts on the systems with  $R =$  Ce, Pr, Nd, Sm, Y, and MM (MM = Ce-rich mischmetal).

TABLE I. Cobalt and iron-rich intermetallic phases in rare earth systems.

Structure Type	at. %Co, Fe	Ce	Pr	Nd	Sm	Gd	Tb	Y	Dy	Er	Tm	Lu
Th <sub>2</sub> Ni <sub>17</sub> , hex	≥89.5	Co Fe	X		X	X	X	X	X	X	X	X
Th <sub>2</sub> Zn <sub>17</sub> , rhomb	89.5	Co Fe	X X	X X	X X	X X	X X	X X	X X			
CaCu <sub>5</sub> , hex	83.3	Co Fe	X	X	X	X	X	X	X	X	X	X
Th <sub>6</sub> Mn <sub>23</sub> , cubic	79.3	Co Fe				X	X	X	X	X	X	X
Gd <sub>2</sub> Co <sub>7</sub> , rhomb.	77.8	Co Fe				X	X	X	X	X	X	X
Ce <sub>2</sub> Ni <sub>7</sub> , hex	77.8	Co Fe	X	X	X	X						
PuNi <sub>3</sub> , rhomb.	75.0	Co Fe	X	X	X	X	X	X	X	X	X	X
MgCu <sub>2</sub> , cubic	66.7	Co Fe	X X	X	X	X	X	X	X	X	X	X

## 1. THE PHASE DIAGRAMS OF THE RARE EARTHS WITH IRON AND WITH COBALT

Most of the rare earth-cobalt alloy systems have been studied in recent years by several laboratories,<sup>(1)</sup> and generally reliable phase diagrams are available for the systems of interest in this investigation. Several rare earth-cobalt phase diagrams are shown in Figure 1. Many of the rare earth-iron systems of interest have also received recent attention,<sup>(2)</sup> but to a lesser extent than the rare earth-cobalt systems. With the exception of  $\text{Y}_2\text{Co}_{17}$ , and possibly  $\text{Sm}_2\text{Co}_{17}$ , all of the  $\text{R}_2\text{Co}_{17}$  and  $\text{R}_2\text{Fe}_{17}$  phases in the present study form by peritectic reaction. Thus, single phase alloys cannot be formed directly from a liquid phase alloy of the correct composition. Either the melted alloy must be cooled slowly through the peritectic reaction or the solidified alloy must be reheated to just below the peritectic temperature to allow the reaction to go to completion. For the  $\text{Nd}_2\text{Co}_{17}$ ,  $\text{Sm}_2\text{Co}_{17}$ , and  $\text{Y}_2\text{Co}_{17}$  phases either technique is satisfactory because the temperature difference between liquidus and peritectic temperature and the composition difference between liquid and intermetallic phase are small. Such is not the case for the other  $\text{R}_2\text{Co}_{17}$  and  $\text{R}_2\text{Fe}_{17}$  phases, however. The temperature difference between the liquidus and peritectic is large, and slow cooling through the liquid plus iron or cobalt range encourages thickening of the peritectic iron dendrites. Thus, below the peritectic temperature, the diffusion distances from the centers of the dendrites are too large to permit the reactions to go to completion at reasonably slow cooling rates. For these alloys, rapid cooling followed by an annealing treatment below the peritectic temperature is the preferred method of preparation. Rapid cooling encourages formation of a fine grained microstructure, shortening diffusion distances and thus the time required for annealing to equilibrium.

## 2. CRUCIBLE MATERIALS

An important factor to consider when preparing rare earth-cobalt, rare earth-iron, or any rare earth-transition metal alloy combination, for

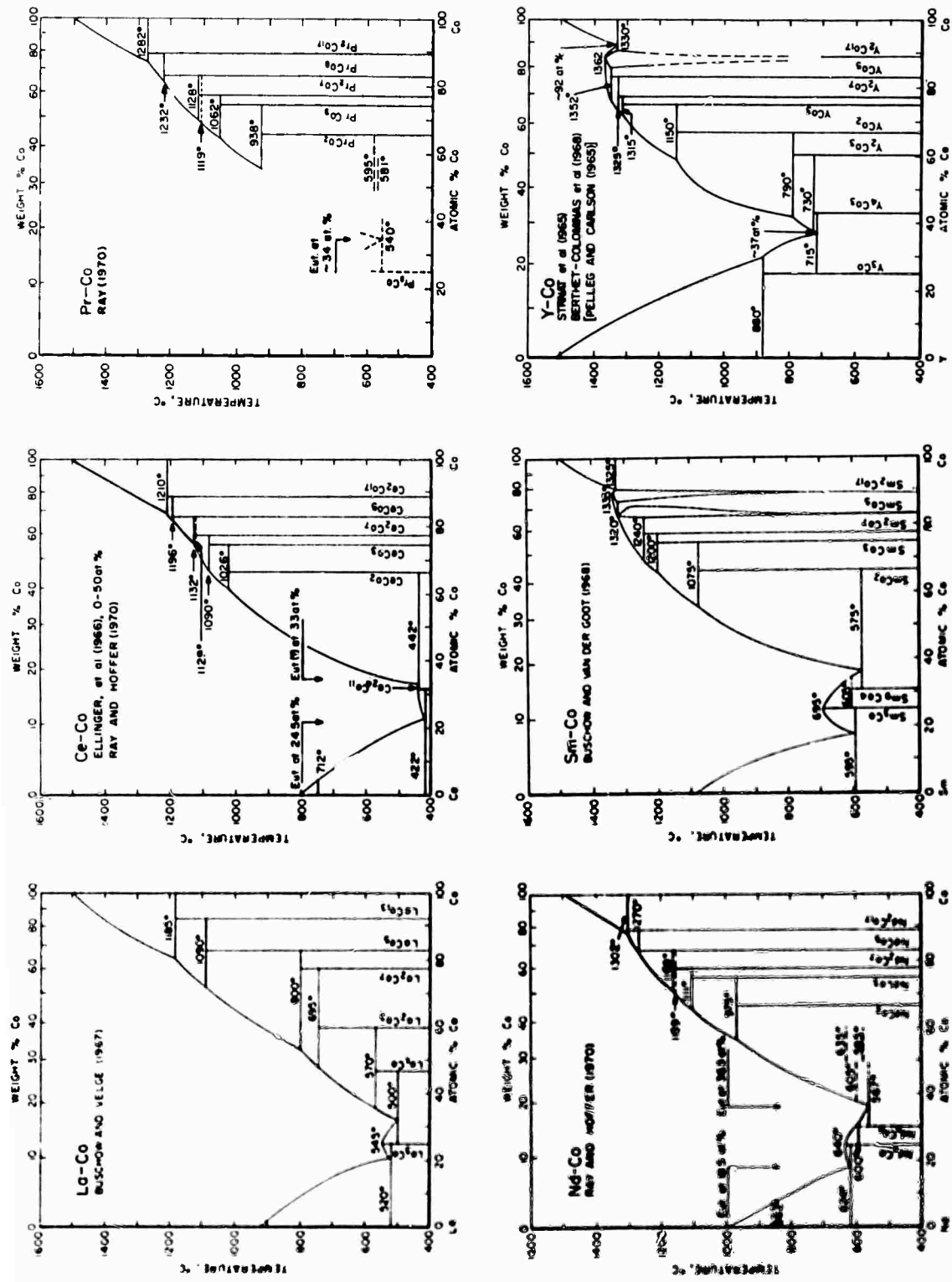


Figure 1. Phase diagrams for six rare earth-cobalt alloy systems.

that matter, are the crucible materials for the alloys. This problem is especially severe for small quantities of alloy, where the surface to volume ratio is large. Tantalum and molybdenum are satisfactory crucible materials for the rare earth metals but they form intermetallic phases with the transition metals. On the other hand, most of the common ceramic oxide materials, e.g., alumina, magnesia, zirconia, etc., make excellent crucible materials for the transition metals but react rather severely with the rare earth metals. The reaction zones between a Pr-Fe alloy and several crucible materials are shown in Figures 2-6. Comparison of these micrographs indicate that yttria ( $Y_2O_3$ ) may be an excellent crucible material for rare earth-transition metal alloys. Unfortunately, yttria crucibles are not commercially available. We have found that flame sprayed  $Y_2O_3$  approximately .010 inch thick onto  $Al_2O_3$  crucibles and thermocouple sheaths works satisfactorily. No spalling of the  $Y_2O_3$  coating has been noted on thermal cycling through  $1500^{\circ}C$ . In lieu of the availability of  $Y_2O_3$  or  $Y_2O_3$ -coated crucibles, the recommended crucible materials would be high density alumina for transition metal-rich alloys and either tantalum or molybdenum for rare earth-rich alloys. Melting and other heat treatments should be done at the lowest practicable temperatures to minimize crucible contamination of the alloys.

### 3. RARE EARTH METALS

Most of the commercially available research quality rare earth metals have stated purities of 99.9+%. This figure is misleading because it does not refer to the total purity level but rather to the purity of the particular rare earth metal with respect to all of the other rare earth metals present. Nonrare earth impurities in the metal may be given separately or not at all. All rare earth metals contain some nonmetallic impurities such as oxygen, nitrogen, and carbon as well as metallic impurities such as magnesium, calcium, iron, etc. The most serious impurity would appear to be oxygen. Any oxygen will be present as a very stable rare earth oxide, and that portion of the rare

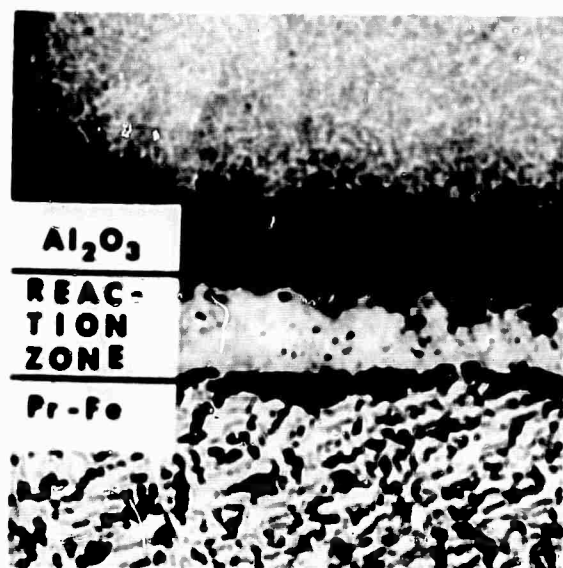


Figure 2. Interface between a Pr-86 at. %Fe alloy and  $\text{Al}_2\text{O}_3$  heated to  $1450^\circ\text{C}$ . 75 X

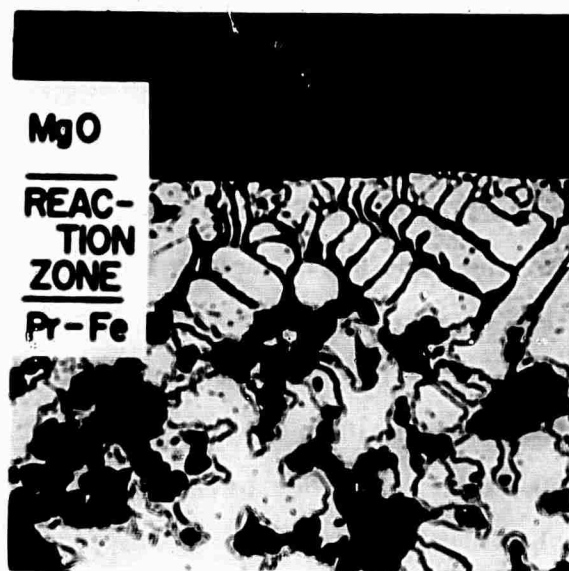
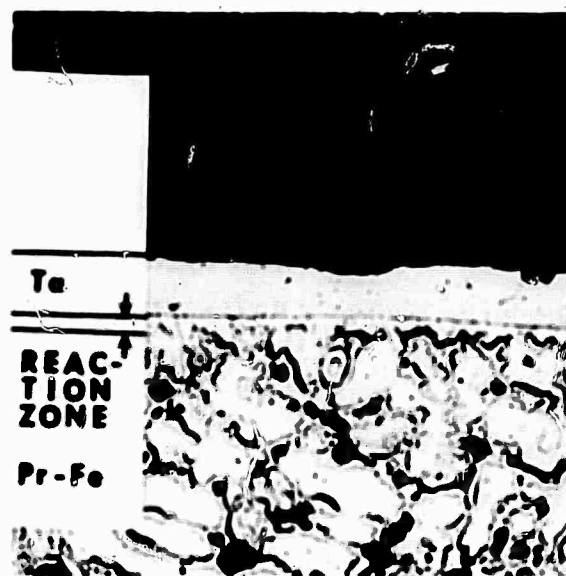


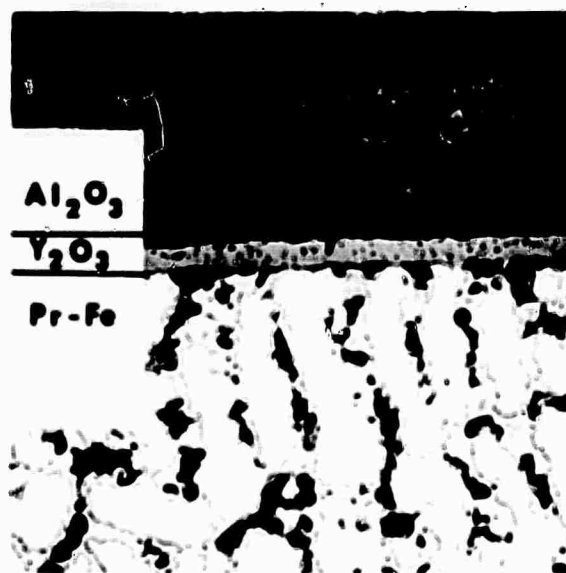
Figure 3. Interface between a Pr-86 at. %Fe alloy and  $\text{MgO}$  heated to  $1450^\circ\text{C}$ . 75 X



Figure 4. Interface between a Pr-86 at. %Fe alloy and  $\text{ZrO}_2$  heated to  $1450^\circ\text{C}$ . 75 X



**Figure 5.** Interface between a Pr-86 at. % Fe alloy and tantalum (Ta) heated to 1450°C. 75 X



**Figure 6.** Interface between a Pr-86 at. % Fe alloy and Y<sub>2</sub>O<sub>3</sub> heated to 1450°C. 75 X



earth present as oxide is unavailable for alloying purposes. There is a rather wide variation in the impurity levels of the various rare earth metals not only from source to source, but also from lot to lot from the same source. We have melted samarium alloys in which as much as 20% of the total weight of the samarium added to the alloy was lost by vaporization during arc melting. Utilizing the same procedures except a different lot of samarium, weight losses less than 0.5% by weight of the samarium present in the alloy have been observed.

It is generally impractical to obtain a separate chemical analysis of the impurities present in each lot of rare earth metal used for alloying purposes. On request, the vendor will generally supply a typical analysis and sometimes even an actual lot analysis of the metallic impurities present. However, the oxygen content is most needed and generally unavailable. Moreover, unless unusual precautions are taken, the oxygen content of the rare earth metal will increase with time.

We determine the amount of rare earth available for alloying experimentally. We first calculate the theoretical stoichiometric weight ratio required to prepare a single phase alloy. We then add excess quantities of rare earth metal to a series of alloys, generally 1, 2, or 3% by weight of the rare earth metal. After melting and homogenization, we determine metallographically which alloy is closest to being single phase. We then correct all alloys made with this lot of rare earth metal accordingly. This procedure needs to be done only once for each lot of material provided reasonable precautions are taken in the storage of the metals and any surface oxide layers are carefully ground away before use in alloying.

#### 4. MELTING PROCEDURES FOR RARE EARTH-TRANSITION METAL ALLOYS

Four melting techniques were considered for the preparation of rare earth-transition metal alloys. These four and their advantages and limitations are compared in Table II. Inert arc melting has been selected as the

**TABLE II**

**Summary of advantages and limitations of melting techniques for research quantities of rare earth-transition metal alloys.**

	<u>Inert Arc</u>	<u>Levitation</u>	<u>Induction</u>	<u>Resistance</u>
<b>Size Limits</b>	5 - 50 grams	1-10 grams	Unlimited	Unlimited
<b>Chance for Crucible Contamination</b>	Negligible	Very Small	Large	Large
<b>Temperature Control</b>	Little	Very Little	Fair	Good
<b>Temperature Measurement</b>	Difficult	Fair	Fair	Good
<b>Heating/Cooling Rates</b>	Fastest	Very Fast	Slow to Fast	Slowest
<b>Uniformity of Heating/Cooling</b>	Poor	Good	Good	Best
<b>Tendency for Directional Solidification</b>	Strong	Controllable	Controllable	Least

principal means of alloy preparation primarily because of the quantity of alloy required (25-40 grams). The amounts needed are larger than is practicable to prepare by levitation melting. On the other hand, serious crucible contamination was feared if alloys in the 25-40 gram range were prepared either by induction melting or in resistant furnaces. Inert arc melting is not without some serious limitations, however. The most serious of these is the strongly directional solidification that is obtained when the molten alloy solidifies on the water-cooled copper hearth. If solidification takes place over a relatively wide temperature range, there is a strong tendency for the higher melting component to solidify near the bottom of the button next to the hearth, with the lower melting components solidifying last toward the top of the alloy button. This tendency to segregate can be minimized by keeping the size of the melt as small as possible. Another problem encountered in arc melting is control of the temperature of the melt. Increasing the intensity of the arc increases the amount of the alloy that is molten at one time which enhances mixing. However, increasing the intensity of the arc also increases the surface temperature of the melt. If one of the alloy components has a high vapor pressure, such as samarium, there is danger in preferentially losing this component by vaporization, thereby changing the overall alloy composition.

The procedure we use for the preparation of the rare earth-transition metal alloys in 25-40 gram quantities is as follows. Predetermined quantities of rare earth and transition metals are placed in the same depression of the copper hearth. We prepare only one alloy at a time because of the danger of fragmentation of the sample either during heating up or cooling down of the alloy after the initial melting. The furnace chamber is evacuated to approximately 0.1 mm Hg and then flushed with an inert gas mixture composed of 75% argon and 25% helium. The evacuation and flushing procedure is repeated three times. The furnace chamber is then brought to a final pressure of 300 mm Hg. Before melting the rare earth-transition metal alloy, a titanium button is held molten for approximately 2 minutes to remove any

reactive gases that may remain in the melting chamber. Finally, the rare earth and transition metals are co-melted. The arc is first directed to the lower melting rare earth point and then the higher melting transition metal is slowly added so that the overall melting temperature of the melt is kept as low as possible to prevent excessive vaporization. A swirling action of the arc around the button gives a stirring action to the melt. After the alloy has been molten for approximately 1 minute, the arc is turned off, the alloy button inverted, and the melting procedure repeated. The total procedure of melting and inversion is repeated 3 to 4 times to insure complete mixing.

5. PROCEDURES FOR THE PREPARATION OF SINGLE PHASE ALLOYS OF  $R_2Co_{17}$ ,  $R_2Fe_{17}$ , AND  $R_2(Co_{1-x}Fe_x)_{17}$

a.  $R_2Co_{17}$  Phases

The  $R_2Co_{17}$  phases with  $R = Ce, Pr, Nd, Sm, Y,$  and  $MM$  can be prepared in 20-40 gram quantities by arc melting followed by a homogenization heat treatment below the peritectic temperature. Component metals are co-melted using a predetermined excess of rare earth to correct for nonrare earth impurities. The amount of excess required ranges from 1 to 3 percent by weight of the rare earth metal. The alloys are inverted and remelted three to four times to enhance homogeneity. After the initial melting, precautions must be taken to prevent the alloys from cooling below red heat during the inversion and remelting procedure. There is a strong tendency for the alloy buttons to shatter on cooling below red heat ( $750-800^{\circ}C$ ). The strong thermal stresses causing the alloy buttons to fragment may be associated with the Curie transformation. The fact that the buttons seldom shatter after the first melting is probably due to incomplete mixing of the components. By the same token, fragmentation on cooling is generally indicative of adequate mixing. Because of the tendency to fragment, it is not advisable to attempt to prepare more than one alloy button at a time.

The appearance of several as arc melted rare earth-cobalt alloys with approximately  $R_2Co_{17}$  stoichiometry are illustrated in Figures 7-9. The differences in these microstructures result from the temperature range between liquidus and peritectic temperature and the composition range between that of the peritectic phase (89.5 at. %Co) and the composition at the intersection of the peritectic line with the liquidus. The latter determines what fraction of the alloy can solidify as free cobalt before the peritectic temperature is reached, while the former determines how long, and thus how thick, the cobalt dendrites can grow before the peritectic reaction begins. The wider either of these ranges, the further the as-cast alloy will be from equilibrium. These temperature and composition ranges narrow from 105°C and 5.5 at. % for Ce-Co, to 40°C and 2 at. % for Pr-Co, to less than 10°C and 1 at. % for Nd-Co. The Ce-Co alloy, Figure 7, is far from equilibrium, showing cobalt dendrites surrounded by  $Ce_2Co_{17}$ . The dark phase surrounding the  $Ce_2Co_{17}$  is mostly  $CeCo_5$ . The Pr-Co alloy, Figure 8, is much closer to equilibrium, with just detectable amounts of free cobalt (1-2%) within the large  $Pr_2Co_{17}$  grains and some  $PrCo_5$  in the grain boundaries. The as arc melted Nd-Co alloy, Figure 9, is entirely single phase  $Nd_2Co_{17}$ , in spite of the fact that  $Nd_2Co_{17}$  forms by peritectic reaction. The microstructure shows that the original cobalt dendrites were narrow enough for the peritectic reaction to go to completion even at the extremely rapid cooling rate.

The arc melted  $R_2Co_{17}$  alloys are homogenized by wrapping the alloys in tantalum foil and heating them for 24-48 hours at 1100°C either in vacuum or an inert atmosphere. The appearance of some homogenized  $R_2Co_{17}$  phases are shown in Figures 10-14. Figure 10 shows a Ce-Co alloy whose composition is slightly to the cobalt-rich side of  $Ce_2Co_{17}$ . The dendritic structure of the excess cobalt has persisted through the homogenization treatment. In contrast, a Ce-Co alloy, slightly cerium-rich from  $Ce_2Co_{17}$  stoichiometry, is shown in Figure 11. In this case, the lower melting  $CeCo_5$  has spheroidized during homogenization. Figures 12 and 13 show

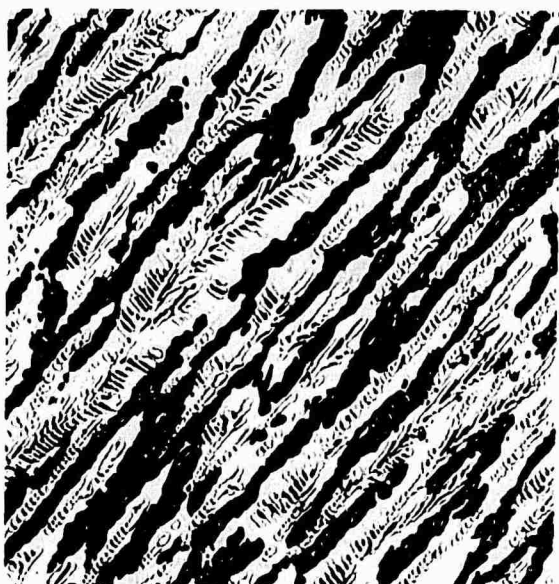


Figure 7. Arc melted Ce-89.5 at. %Co alloy. Cobalt dendrites peritectically surrounded by  $\text{Ce}_2\text{Co}_{17}$ . The dark phase is  $\text{CeCo}_5$ . 250 X



Figure 8. Arc melted Pr-89 at. %Co alloy. This alloy is primarily  $\text{Pr}_2\text{Co}_{17}$  with some  $\text{PrCo}_5$  and just detectable amounts of free cobalt. 250 X



Figure 9. Arc melted Nd-89 at. %Co alloy. This alloy is essentially single phase  $\text{Nd}_2\text{Co}_{17}$  even though  $\text{Nd}_2\text{Co}_{17}$  forms by peritectic reaction. 250 X

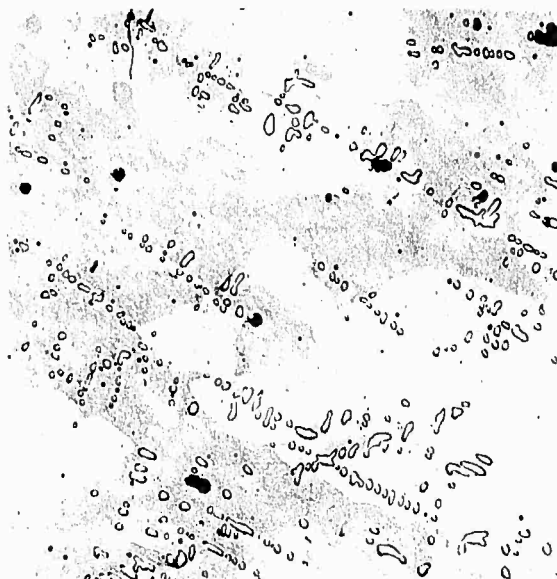


Figure 10. Ce-89.5 at. %Co homogenized  
32 hours at  $1100^\circ\text{C}$ .  $\text{Ce}_2\text{Co}_{17}$   
with excess cobalt as dendrites.  
250 X

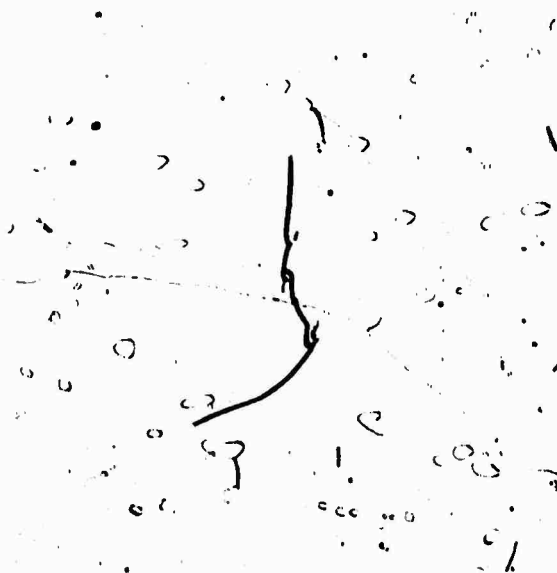


Figure 11. Ce-89 at. %Co homogenized  
50 hours at  $1100^\circ\text{C}$ .  $\text{Ce}_2\text{Co}_{17}$   
with excess cerium as  $\text{CeCo}_5$ .  
250 X



Figure 12. Pr-89 at. %Co homogenized 50 hours at 1100°C. Single phase  $\text{Pr}_2\text{Co}_{17}$ , light and dark regions are annealing twins. 250 X

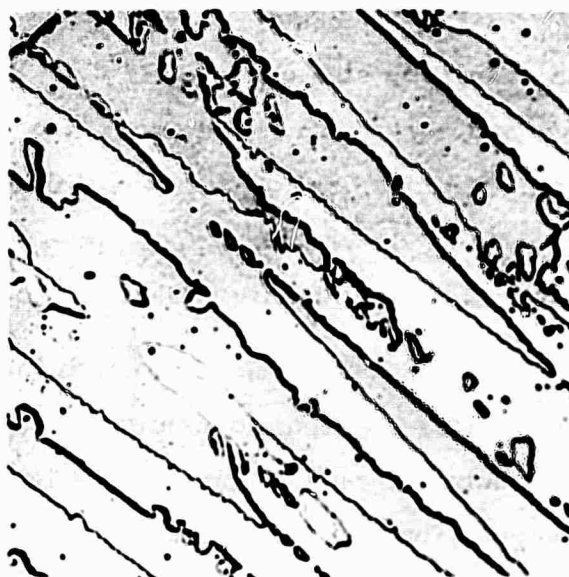


Figure 13. Nd-89 at. %Co homogenized 50 hours at 1100°C. Single phase  $\text{Nd}_2\text{Co}_{17}$ . 250 X.

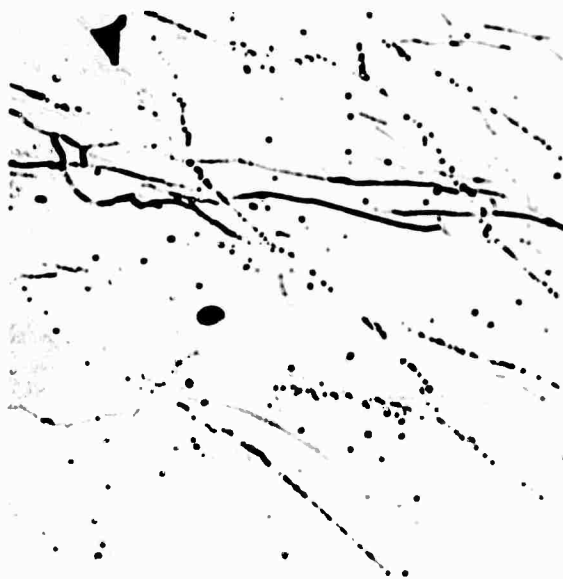


Figure 14. Y-89 at. %Co homogenized 50 hours at 1100°C.  $\text{Y}_2\text{Co}_{17}$  plus an unidentified phase segregated to the grain boundaries. It is suspected this second phase material was carried over from the yttrium used for alloying. 250 X



homogenized, single phase  $\text{Pr}_2\text{Co}_{17}$  and  $\text{Nd}_2\text{Co}_{17}$  alloys, respectively. The light and dark contrasting areas are annealing twins formed by these phases during homogenization. X-Ray diffraction patterns of the Y-Co alloy, Figure 14, shows only  $\text{Y}_2\text{Co}_{17}$  present. The dark phase in the grain boundary is probably an impurity phase.

Most of the rare earth metals are purified to a certain extent during arc melting. A slag, presumably a rare earth oxide, floats on top of the alloy button during melting where it remains on solidification. Slagging is not observed for yttrium or yttrium alloys. The impurity, probably yttrium oxide, segregates at the grain boundaries of the alloy. The apparent pinning of the grain boundaries by the impurity phase makes it very difficult to break down the as-cast microstructure of yttrium alloys by homogenization.

#### b. $\text{R}_2\text{Fe}_{17}$ Phases

Our first attempts to prepare  $\text{R}_2\text{Fe}_{17}$  phases with  $\text{R} = \text{Ce}, \text{Pr},$  or  $\text{Nd}$  by arc melting, or any other method, were frustrated by gross segregation of the alloys during solidification. An as arc melted Ce-89 at. % Fe is shown in Figure 15. The button is divided into two distinct layers. The bottom portion of the button contains thick iron dendrites surrounded by  $\text{Ce}_2\text{Fe}_{17}$ . At the center of the micrograph, the microstructure changes sharply to very fine iron dendrites surrounded by a thick layer of  $\text{Ce}_2\text{Fe}_{17}$  plus a dark phase. Although the magnification is not sufficiently large to show the detail, the  $\text{Ce}_2\text{Fe}_{17}$  is surrounded by a thin shell of  $\text{CeFe}_2$  and the dark phase is the Ce-Fe eutectic. On homogenization for 8 hours at  $875^\circ\text{C}$ , a similar Ce-Fe alloy has the microstructure shown in Figure 16. The top portion of the button is essentially single phase  $\text{Ce}_2\text{Fe}_{17}$ , while the bottom portion is about 50% iron dendrites in a matrix of  $\text{Ce}_2\text{Fe}_{17}$ . Similar behavior is observed for Pr-Fe and Nd-Fe alloys.

The sources of the gross segregation are probably liquid miscibility gaps existing above the  $\text{R}_2\text{Fe}_{17}$  compositions. The volume of iron-rich portion can be varied by shifting the overall alloy composition, but the



**Figure 15.** Arc melted Ce-89 at. % Fe showing gross segregation which develops on solidification. The average composition of the bottom portion (thick dendrites) is about 95 at. % Fe, the top portion about 87.5 at. % Fe. 50 X



**Figure 16.** Ce-89 at. % Fe homogenized 8 hours at 875°C, showing how the gross segregation developed on solidification (Figure 15) persists after homogenization. The top portion of alloy is essentially single phase Ce<sub>2</sub>Fe<sub>17</sub> while the bottom portion is iron in a matrix of Ce<sub>2</sub>Fe<sub>17</sub>. 50 X

composition within either segregated area appears to remain constant. It is estimated that the iron-rich material contains 95-96 at. %Fe while the rare earth-rich volume contains about 87.5 at. %Fe. In order to completely eliminate the gross segregation of the Ce-Fe, Pr-Fe, and Nd-Fe alloys, the overall alloy composition must contain less than 87.5 at. %Fe. Since  $R_2Fe_{17}$  stoichiometry is 89.5 at. %Fe, an alloy containing less than 87.5 at. %Fe will contain excess rare earth. An example of a Pr-87 at. %Fe alloy homogenized 8 hours at  $1000^{\circ}C$  is shown in Figure 17. Large, twinned grains of  $Pr_2Fe_{17}$  are observed along with dark voids which were originally filled with the Pr-Fe eutectic ( $Pr + Pr_2Fe_{17}$ ). (The praseodymium oxidizes readily during polishing and etching and the eutectic material has fallen out.)

Since any free iron present would interfere with the evaluation of the  $R_2Fe_{17}$  alloys, it is necessary that these alloys be prepared on the rare earth-rich side of  $R_2Fe_{17}$  stoichiometry. For Pr-Fe and Nd-Fe alloys this is not a serious problem because  $Pr_2Fe_{17}$  and  $Nd_2Fe_{17}$  are the only intermediate phases in the respective systems, and the excess rare earth can be oxidized away. Excess cerium in Ce-Fe alloys, however, will be present as  $CeFe_2$ .  $CeFe_2$  is ferromagnetic and a possible source of interference during magnetic measurements.

$R_2Fe_{17}$  with  $R = Ce, Pr,$  and  $Nd$  are prepared by arc melting alloys containing from 87 to 87.5 rather than 89.5 at. %Fe. The arc melted alloys are then wrapped in tantalum foil and homogenized at  $800-900^{\circ}C$  for 4 to 24 hours. Alloys prepared in this manner are slightly rare earth-rich.

The liquid miscibility gap problem apparently does not exist for  $R_2Fe_{17}$  phases with  $R = Sm, Y,$  or  $MM$ , and these alloys can be prepared as the  $R_2Co_{17}$  phases.

#### c. $R_2(Co_{1-x}Fe_x)_{17}$ Phases

Single phase alloys of the type  $R_2(Co_{1-x}Fe_x)_{17}$  can be prepared by essentially the same manner as described for the  $R_2Co_{17}$  phases for all



**Figure 17.** Pr-87 at. % Fe homogenized 8 hours at 1000°C. Large grains of  $\text{Pr}_2\text{Fe}_{17}$ , some heavily twinned, with dark voids which originally contained Pr +  $\text{Pr}_2\text{Fe}_{17}$  eutectic. 250 X

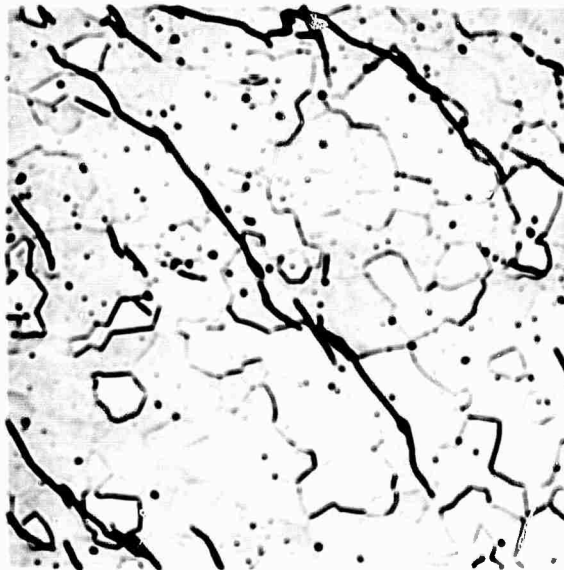


**Figure 18.**  $\text{MM}_2(\text{Co}_{.75}\text{Fe}_{.25})_{17}$  alloy homogenized 50 hours at 1100°C. 250 X

values from  $x = 0$  to  $x = 1$  for alloys with  $R = \text{Sm, Y, and MM}$  and for  $R = \text{Ce, Pr, Nd}$  for  $x \leq 0.5$ . A single phase alloy with the composition  $\text{MM}_2(\text{Co}_{.75}\text{Fe}_{.25})_{17}$  is shown in Figure 18. This alloy was prepared by co-arc melting stoichiometric quantities of MM, Co, and Fe plus a predetermined excess of MM (in this case 2.5 weight percent over the stoichiometric amount). The arc melted alloy was then homogenized in vacuum at  $1100^\circ\text{C}$  for 48 hours.

We have not successfully prepared single phase alloys of  $\text{R}_2(\text{Co}_{1-x}\text{Fe}_x)_{17}$  for  $R = \text{Ce, Pr, or Nd}$  with  $x > 0.5$ . Such alloys could probably be prepared by mixing single phase  $\text{R}_2\text{Co}_{17}$  and  $\text{R}_2\text{Fe}_{17}$  powders and hot pressing the mixture in a vacuum or inert atmosphere. This technique would avoid the liquid immiscibility problem by eliminating the need to melt the component elements.

## SECTION II

### DIFFERENTIAL THERMAL ANALYSIS APPARATUS

#### I. INTRODUCTION

Differential Thermal Analysis or DTA is one of the most important tools in the study of structural changes in metals and alloys, since it permits the detection of any process which involves evolution or adsorption of latent heat. The present equipment has detected changes in the magnetic state of metals and alloys between  $300^{\circ}\text{C}$  and  $900^{\circ}\text{C}$ , and also allotropic transformations and peritectic decomposition reactions up to  $1550^{\circ}\text{C}$ . Current trends to higher temperatures have necessitated sensors which will withstand high temperature attack of reactive metal vapors for sustained periods of time. The thermocouple combination W 25% Re vs doped W 3% Re (Engelhard Industries) has been found to withstand such exposures successfully despite embrittlement. Maximum temperatures of  $1650^{\circ}$  -  $1700^{\circ}\text{C}$  have been reached.

Endothermic or exothermic reactions occurring within the specimen are reflected in a lower or higher temperature of the specimen junction relative to the inert reference material (Pt) junction.

The following conditions provide reproducibility and high sensitivity in recording DTA events.

- a. Existence of a smooth temperature gradient from heat source to heating block to specimen and within the specimen itself. (Specimen temperature and reference temperature are measured on the axis of cylindrical samples and which are symmetrically located with heating block.)
- b. A smooth linear rate of change of furnace temperature by a controller-programmer.
- c. Excellent thermal insulation on top and on the bottom of the heater block so as to maintain the smooth gradient across the block.

- d. Calibration tests were conducted on selected materials which undergo reproducible crystallographic transformations. Iron has well-known transition and fusion temperatures covering a range from approximately 1550°C.

Table III shows the calibration tests made to date.

## 2. COMPONENTS

### a. Thin Film Evaporator

The DTA module is housed inside the belljar of a Veeco High Vacuum Thin Film Evaporator, Model VE-770. This apparatus provides the necessary vacuum requirements prior to inert gas backfilling. It consists of standard components capable of providing  $10^{-7}$  to  $10^{-9}$  mm Hg pressure. A special 20 inch diameter baseplate accommodates the power entry to the resistance heater from the bottom and also to accommodate the Stupakoff seals for water, inert gas, and thermocouple leads.

A water-cooled baffle is located between the 10 inch diffusion pump and the liquid nitrogen cold trap. Backstreaming diffusion pump oil is condensed on the internal water-cooled baffle surfaces and returned to the diffusion pump.

### b. DTA Module

The module consists of the following components (refer to Figure 19).

- (1) Three legs support a water-cooled copper enclosure on the baseplate. The enclosure is situated between the terminal posts which transfer power to the resistance heater.
- (2) The single phase tungsten resistance element is 1-1/2 inches ID by 3 inches high. The total length of electrodes with body is 7-1/4 inches. The heater is tungsten mesh, fabricated by Sylvania Electric Products. The mesh consists of interlocking wire coils which provide flexibility after recrystallization of the metal, thus preventing breakage.

TABLE III  
Calibration DTA apparatus

Observed transition temperature °C							Literature Metals Handbook
EVENT	AISI Iron* Bar 114A			High Purity Iron (99.98%) Bram Metallurgical & Chem. Co.			
	UDTA No. 56 (12-30-70)			UDTA No. 53 (12-15-70)			
	HEAT	COOL	AVG.	HEAT	COOL	AVG.	Average of 4 observations
Curie	769	772	770.5	768	772	770.0	770
α to γ	913	909	911.0	911	906	908.5	910
γ to δ	1392	1390	1391.0	1403	1401	1402.0	1400
Melting Point	1535	1532	1533.5	1533	1528	1530.5	1535
T max	1614	Eutectic Cu + 8.5 w/o Al.			1550		
	UDTA No. 3						
Eutectic	1039	1035	1037				1037
CONDITIONS:							
5 gms specimen (cylindrical slug)							
7 gms platinum reference							
0 °C cold junction for specimen thermocouple							
Thermocouples	W 25% Re vs W 3% doped Re - heating: 5.5 °C min						
	1 Atm He-Ar Rate of cooling: 5.0 °C min						
* Total nonmetallic impurities 4 ppm; total detected metallic impurities 32 ppm.							



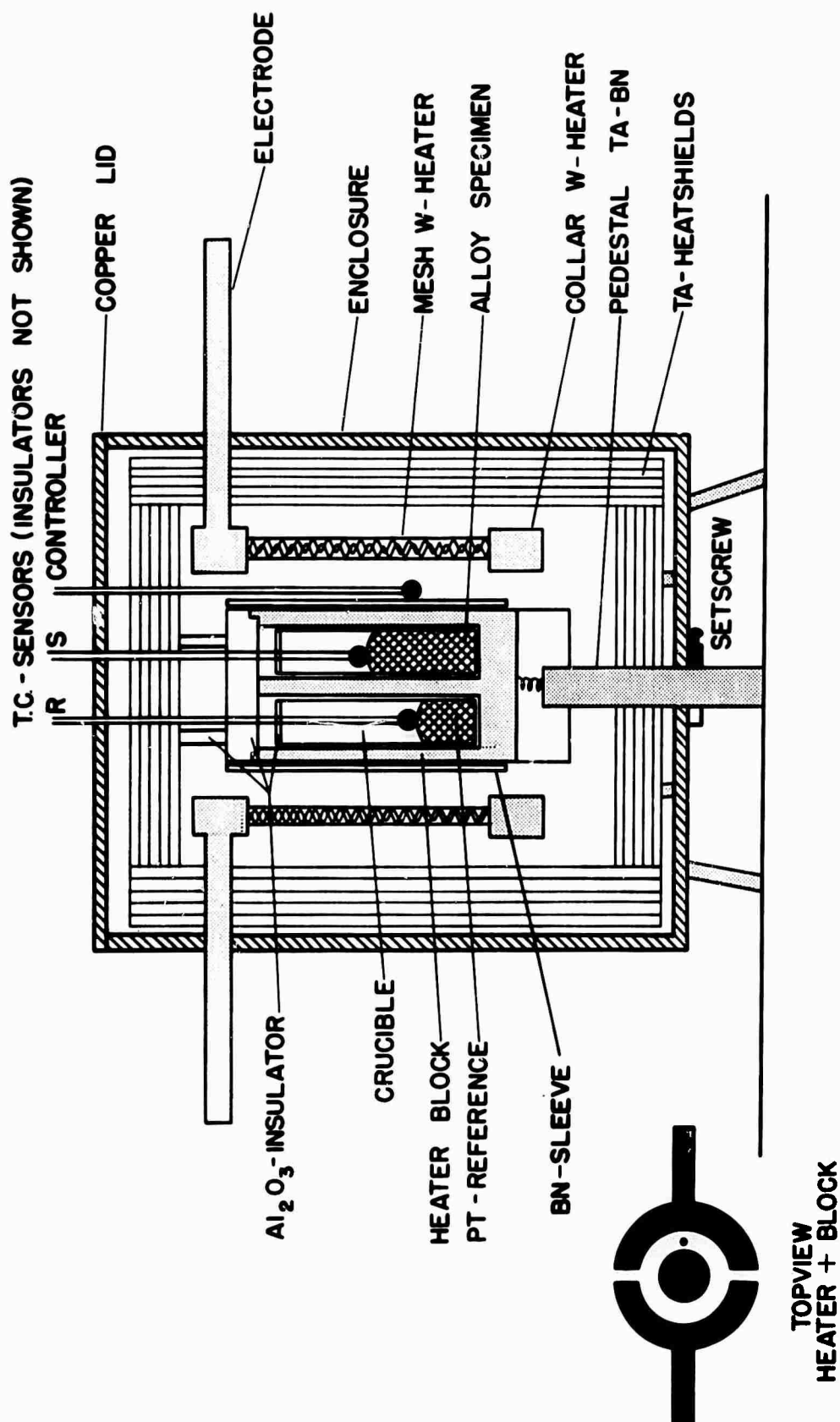


Figure 19. DTA Module.

- (3) The heat shield assembly is situated between the heater and the copper enclosure. The shields are made of tantalum and consist of six concentric cylinders, held together by tantalum pins. Top and bottom heat shields are also made of six-layered tantalum sheet. They were also fabricated by Sylvania. The two inner heat shields are removable, providing a means for varying the thermal gradient.
- (4) The tungsten heating block and its tantalum-boron nitride pedestal were made in this laboratory. The cavities were machined to accommodate standard-sized high purity  $\text{Al}_2\text{O}_3$  (or MgO) crucibles. A boron nitride sleeve was introduced to maintain a  $75^\circ\text{C}$  thermal differential between the specimen and heater. Insulators around thermocouple leads and on top of the block provide further controls for proper heat flow across the block.

c. Solid State Temperature Controller

The THERMAC Solid State Temperature Controller, Model TC 5192 provides the means for establishing and automatically maintaining the temperature of a workpiece at any selected setpoint level within the operating range of the system, which is between  $400^\circ\text{C}$  and  $1800^\circ\text{C}$  limited by the thermocouple combination W-Re. An alternate operating mode in addition to setpoint control is used in the DTA setup. The workpiece temperature is programmed into the system whereby the heater voltage is dictated by automatic time-temperature programming through the DATA-TRAK Programmer output potentiometer which provides the command signal.

The controller thermocouple in Figure 19 is connected to the temperature controller.

d. Programmer

The DATA-TRAK Curve-Following Programmer, Model FGE 5110 employs an electrostatic curve following system which provides positioning of the shaft of a rotary output potentiometer in accordance with variations in a preplotted program, attached to a rotating drum. A desired program curve is etched in the metallized surface of a program chart. The chart is then mounted on the outer surface of the program drum, which is installed in the DATA-TRAK. The two isolated planes on the surface of the chart are separately energized by oppositely phased a-c voltages applied through insulated hubs of the program drum. These voltages established an electrostatic voltage gradient across the gap on the chart created by the program curve. As the drum rotates the chart past the curve following probe to seek the zero potential existing at the center of the program curve, the shaft of an output potentiometer, mechanically coupled to the probe through pulleys, is turned. The potentiometer transfers the command signal to the solid state controller.

Various program charts have been prepared allowing heating and cooling rates from  $0.5^{\circ}\text{C}/\text{minute}$  to  $> 50^{\circ}\text{C}/\text{minute}$ . The DATA-TRAK is made by Research, Inc.

e. Saturable Core Reactor

The Fincor Self-Saturating Reactor, Leeds & Northrup Catalog No. FCG1 provides the advantages of proportional, reset, and rate actions for stepless regulation of the electric power which is directed to the transformers.

Any deviation from a selected setpoint is determined at the same time as an error signal. Depending upon the error direction, magnitude, and duration, the output is corrected by a current adjusting type unit which drives a saturable core reactor through a magnetic amplifier. The correct power input is supplied to the load.

f. Transformers

Two Hevi Duty Electric Company transformers are used with the following specifications: 5.0 KVA, 60 Cycle, 120/240 V, single phase.

Transformer output is directed to the W resistance heater through heavy water-cooled copper wire cables.

g. X-Y Recorder

Graphic reproduction of the thermocouple signals is accomplished with a Honeywell 560 X-Y recorder.

The specimen temperature is recorded on the X-axis while the differential temperature between reference and specimen is recorded on the Y-axis ( $\Delta T$ ). Details of the circuits are shown in Figure 20. The use of a differential thermocouple, rather than simply measuring the temperature change in the specimen alone, provides the advantage of an increase in sensitivity derived from the large expansion of the temperature scale in a difference measurement. To obtain very high sensitivity, the differential thermocouple output must be magnified with a high gain, low noise amplifier which is free from drift. In our measurements, we utilized the 50  $\mu\text{V}/\text{inch}$  sensitivity scale on the Y-axis. The specimen temperature was recorded at 2 mv/inch sensitivity. Further improvements in shielding will be made to overcome stray signals at high sensitivity Y-settings.

h. Inert Gas Purification Train

The 75% Ar-25% He (AIRCO 75) inert gas mixture used for back-filling of the belljar is led over titanium chips heated to 800°C then through a liquid nitrogen trap filled with glass beads to obtain adequate surface area for condensation of impurities in the inert gas. (See Figure 21).

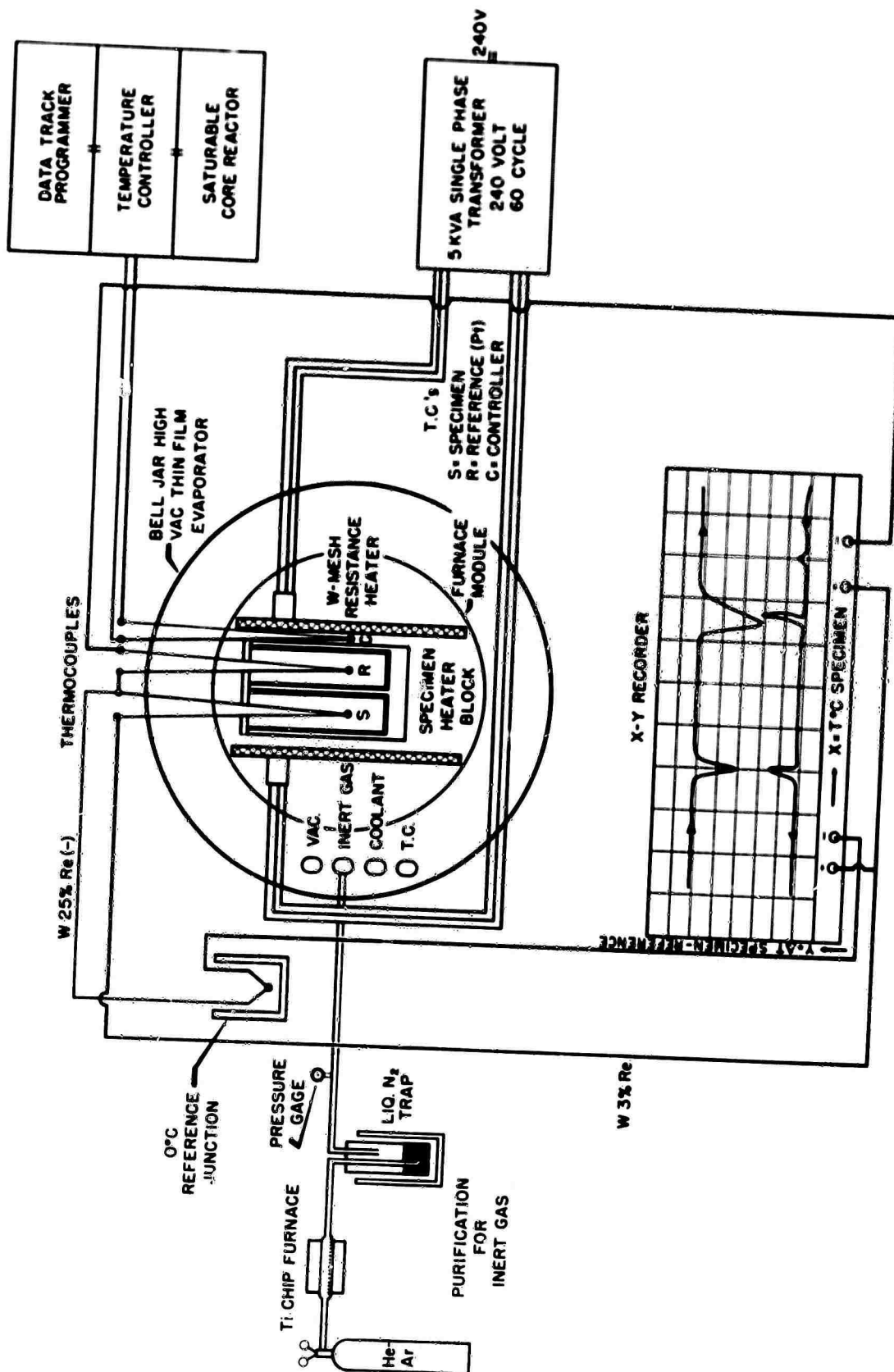


Figure 20. DTA circuits and components.

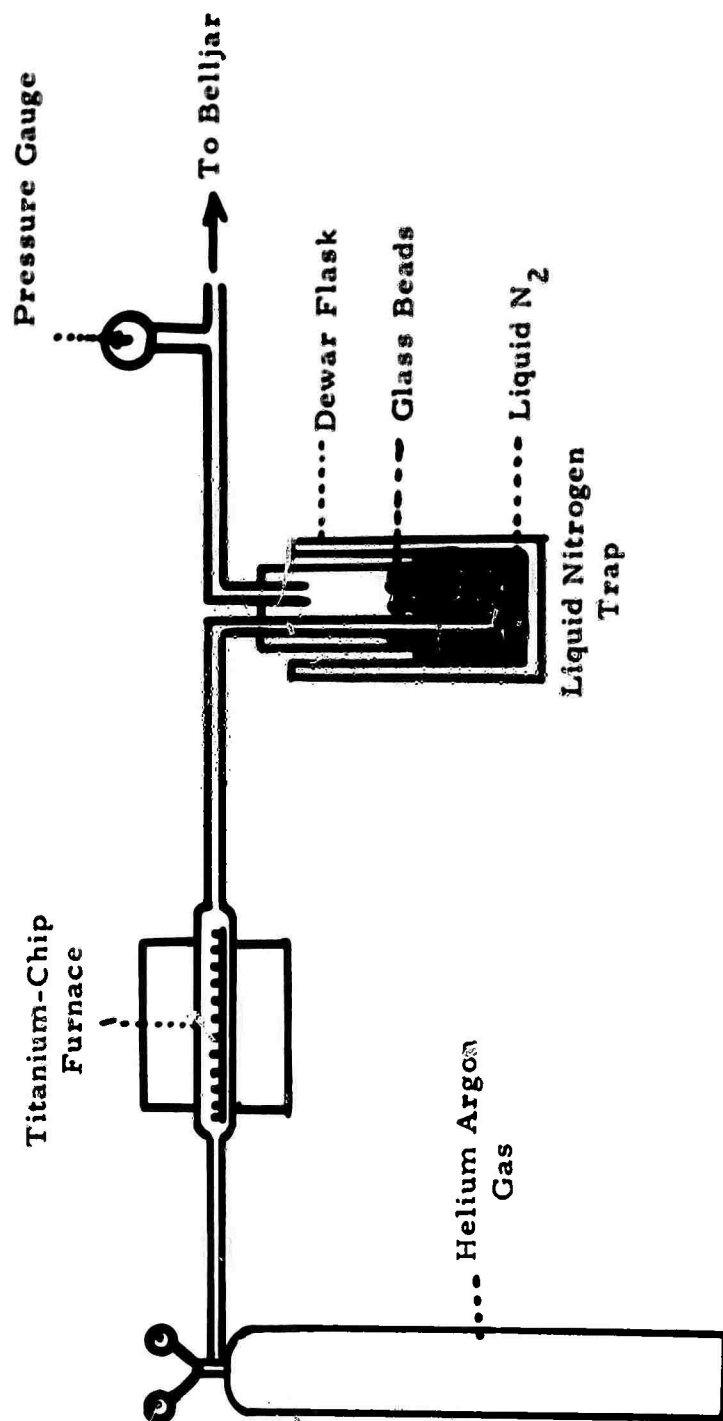


Figure 21. Inert gas purification.

### SECTION III

#### DIFFERENTIAL THERMAL ANALYSIS OF SOME $R_2Co_{17}$ PHASES

Liquidus, peritectic, and Curie temperatures of the  $R_2Co_{17}$  phases prepared in this study were measured with the differential thermal analysis apparatus described in Section II. The values obtained are compared with previously reported data in Table IV.

It is encouraging that the Curie temperature of  $MM_2(Co_{.75}Fe_{.25})$  is  $791^{\circ}C$ , only  $50^{\circ}C$  lower than  $MM_2Co_{17}$ . The Curie temperature of  $MM_2Fe_{17}$  has not been measured, but it is probably not higher than  $0^{\circ}C$ .

TABLE IV

Curie temperatures, peritectic, liquidus, and melting temperatures for some  $R_2Co_{17}$  phases determined by DTA in this investigation compared with previous work.

Phase	Curie Temperature, °C		Peritectic Temperature		Liquidus or Melting Temperature	
	This Work	Previous Work	This Work	Previous Work	This Work	Previous Work
$Ce_2Co_{17}$	801	795 <sup>(3)</sup> 811 <sup>(4)</sup>	1206	1210 <sup>(1)</sup>	1289	1310 <sup>(1)</sup>
$Pr_2Co_{17}$	890	887 <sup>(3)</sup> 898 <sup>(4)</sup>	1265	1282 <sup>(1)</sup>	1327	1320 <sup>(1)</sup>
$Nd_2Co_{17}$	910	893 <sup>(3)</sup> 877 <sup>(4)</sup>	1297	1302 <sup>(1)</sup>	1321	1310 <sup>(1)</sup>
$Sm_2Co_{17}$	925 920	923 <sup>(3)</sup> 917 <sup>(4)</sup>	1316	Congruent <sup>(5, 6)</sup>	1386	1335 <sup>(5)</sup> 1375 <sup>(6)</sup>
$Y_2Co_{17}$	916	940 <sup>(3)</sup> 883 <sup>(4)</sup>	Congruent Congruent <sup>(7)</sup>		1359	1362 <sup>(7)</sup>
$MM_2Co_{17}$	841	-	1219	-	1279	-
$MM_2(Co_{.75}Fe_{.25})_{17}$	791	-	1193	-	1300	-



## SECTION IV

### DESIGN AND CONSTRUCTION OF A

### HIGH TEMPERATURE-HIGH VACUUM TUBULAR FURNACE

#### 1. INTRODUCTION

In the development of rare earth-cobalt magnets and in related research on the  $R_2Co_7$ ,  $RCo_5$ ,  $R_2Co_{17}$  and similar intermetallic compounds, it is necessary to pursue several areas of experimental investigation which require closely controlled heating of samples to high temperatures. Examples of such tasks are the annealing of the alloys, sintering processes, single crystal growing, thermomagnetic analysis (e. g., Curie point measurements), and investigations of the temperature dependence of other physical properties, such as the electrical resistivity. With a view toward the tasks listed above we have designed and fabricated a suitable high temperature-high vacuum tubular furnace system precisely controllable and adaptable for each of these functions.

#### 2. GENERAL DESCRIPTION

The furnace system described herein is illustrated in Figure 22 and can be represented by the simplified block diagram of Figure 23. A compatible arrangement of the various functions of the system relating to power and temperature controls, furnace movement, and vacuum pumping was developed in line with the intended applications. The functional components of the system are described individually in the following.

##### a. Furnace

The tubular furnace selected for the system (Marshall Model 1448) has an inside bore of 2-1/2 inches and a heated length of 28 inches. Overall dimensions of the furnace are 12 inches outside diameter by 36 inches in length. The heating element is made from a multiple-strand platinum-40 % rhodium alloy wire rated for continuous operation at 1540°C. A series of

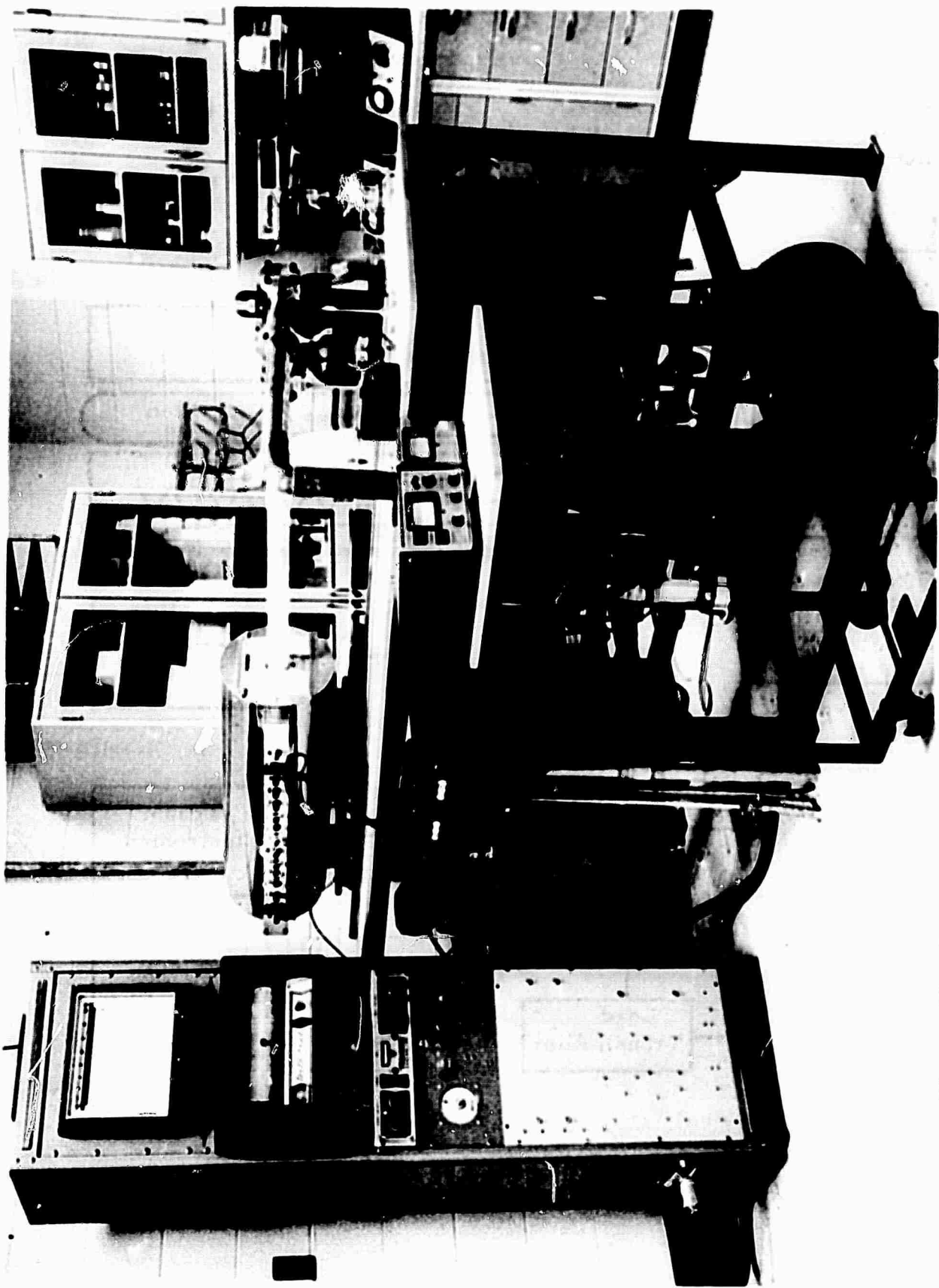


Figure 22. Overall view of high temperature-high vacuum furnace system.

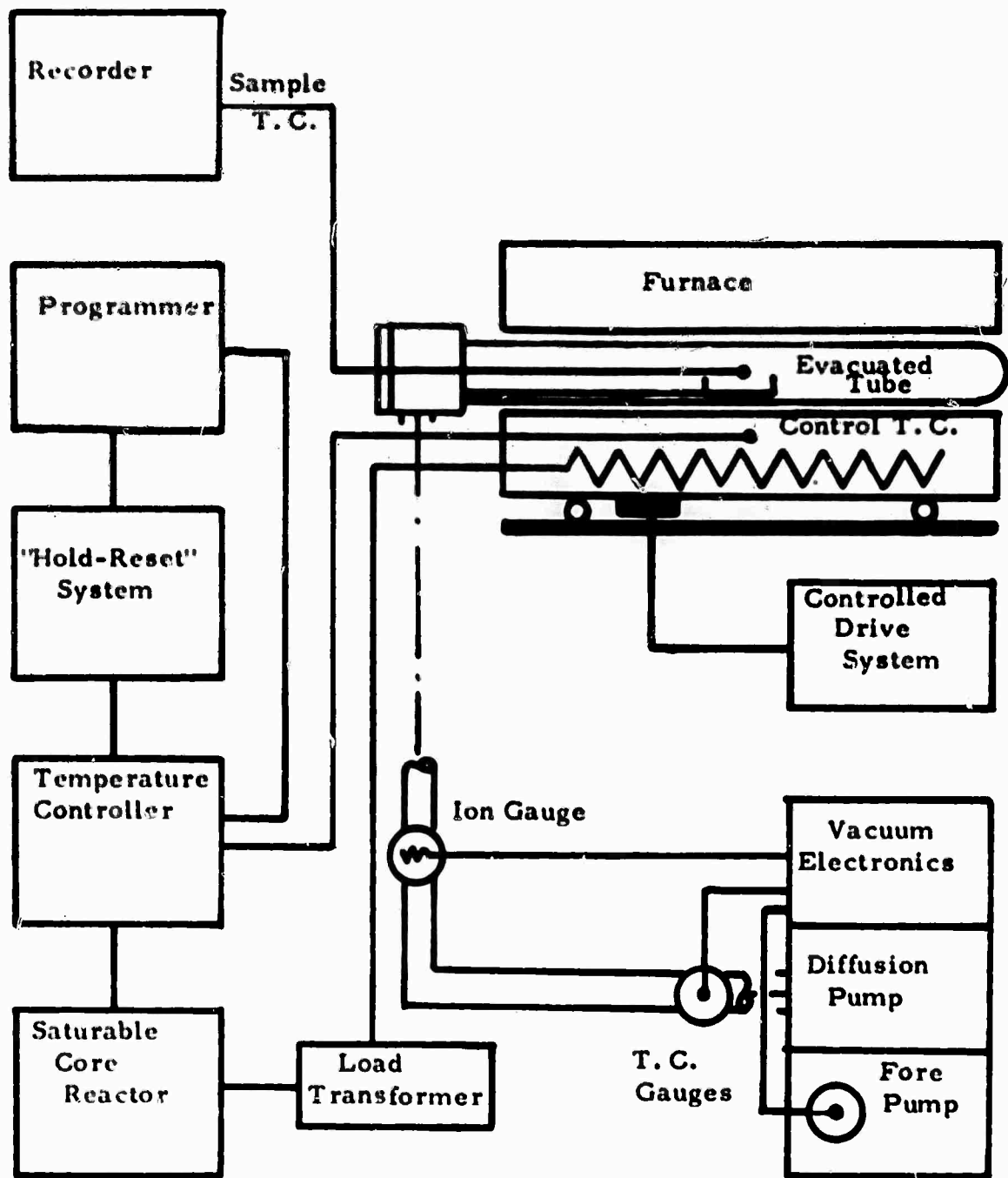


Figure 23. Block diagram, high temperature-high vacuum furnace system.

10 taps are spaced on the element for adjusting the axial temperature distribution in the furnace for a uniform heating field or a specified temperature gradient by means of external shunts. In anticipation of initial applications for homogenization annealing and sintering, the shunts were optimized for a long uniform temperature profile. The temperature over the central 16 inches of the heating zone has been adjusted to be within  $\pm 2^{\circ}\text{C}$  of a set temperature level near  $1000^{\circ}\text{C}$ .

b. Electrical Temperature Control System

In order to achieve the flexibility and precision of control desired for the time dependence of the furnace temperature - while satisfactorily protecting the furnace during operation - an integrated system of high quality commercial control and monitoring equipment was assembled in a standard enclosure.

The primary control device in the system is the temperature controller (Research Incorporated, 5192 THERMAC). A shielded platinum/platinum-13% rhodium control thermocouple located midpoint in the furnace near the heating element is used to develop a feedback signal representative of the furnace temperature. Depending on the mode of controller operation - either manual, setpoint, or remote command - a power controller (Leeds & Northrup Saturable Core Reactor) will respond to a demand for more or less power with respect to a set temperature level. In the manual position, heating element voltage can be varied from the control console independent of the temperature of the furnace. In the setpoint mode, automatic control of the power required to maintain a setpoint level can be achieved. In the manual or the setpoint modes the control accuracy is equivalent to  $\pm 0.25\%$  full scale ( $1500^{\circ}\text{C}$ ) with a repeatability of 0.1%.

In the remote command mode, automatic programming of the power controller is achieved by means of a preplotted chart representing the temperature profile features desired as a function of time. The programmer (Research Incorporated DATA-TRAK Model FGE 5110) has a repeatability of

0.05% with a dead band of 0.01% if a chart range covering 1500°C is used.

This of course is with respect to the control contour plotted on the charts.

Extended operation at a given point, i. e. , a temporary suspension of the precharted program, can be achieved by a "hold" feature, and the desired holding time can be controlled by an auxiliary timing unit built into the control system.

Regardless of the mode of operation, the saturable core reactor controller responds to the magnitude of the positive control signal by applying a proportional voltage to the heating element of the furnace. To match the reactor output (187 volts) to the furnace (154 volts maximum), a step down lead transformer (Marshall fabricated, turns ratio 1:0.825, 6 KVA is incorporated to limit the maximum controlled power that can be supplied to the furnace.

Sample temperatures inside the evacuated Mullite tube are measured by means of Pt/Pt-13%Rh thermocouples (8 or 10 mil wire diameter) brought out through a vacuum seal at the supported end. Temperature monitoring is performed with a strip chart recorder (Leeds & Northrup, Speedomax W) with a full-scale range of 1600°C and chart speeds of 1/2 and 6 inches per hour.

### c. Vacuum System

The vacuum system, also illustrated in Figure 22, consists of a roughing pump (Leiman IPC-6, 6 ft<sup>3</sup>/min), and a high vacuum system (Vacronic "Compact Line"). The vacuum console is plumbed to the furnace stand through 2 inch I. D. copper tubing. "O"-ring-sealed flanges are used to connect the pumping system to the Mullite tube. Graded metal-to-glass seals join the flanges to the tubing. The furnace tube terminates in a matching flange connected to the Mullite with a glass-to-ceramic graded seal. The water-cooled diffusion pump achieves a vacuum of  $1 \times 10^{-5}$  Torr in relatively short pumping periods (15-20 minutes with the empty furnace tube at room temperature or at 1375°C). The pumping speed of the system has proven adequate to rapidly eliminate vapors produced in the outgassing during initial sintering

stages of pressed powder magnets of several cubic centimeters total sample volume. Better ultimate vacua, down to  $10^{-6}$  Torr, may be achieved when use is made of a liquid nitrogen vapor trap incorporated in the diffusion pump stand.

High and low vacuum pressure transducers permit monitoring of the system pressures at critical points during operational procedures. The forepump pressure and relatively poor system vacua are monitored with two standard thermocouple gauges (Vactronic T6-Gc), and the high vacuum with an ion gauge (Bayard-Alpert).

#### d. Furnace Drive System

Utilizing the furnace system for experimental work in single crystal growing or solid state refining tasks requires that a precise temperature gradient be established in the sample and maintained while the mean sample temperature is slowly lowered through an interval. To permit such experiments with our furnace, an electromechanical drive system has been incorporated which can be used to move the furnace along its axis at very slow speeds, thereby withdrawing it from the Mullite tube containing a test sample. To make the slowest speeds meaningful, jerky motion of the furnace, mechanical vibrations causing a relative motion between sample and furnace, and time fluctuations of the temperature must be kept at a minimum. To this end, the forepump and the furnace rack were separated and uncoupled, and the temperature control and mechanical drive components were carefully selected for their consistency with these demands.

The drive system as shown in Figure 24 consists of a constant-torque electronic speed controller (Bodine Model 905) which furnishes power to a d. c. motor (Bodine, NSH-34 RH). The speed range of the motor output shaft can be varied from 1.5 to 56 rpm. The motor drive is coupled through a variable ratio speed reducer (Geartronics Model 2601, reduction range 1-1000) to a standard precision lead screw (Wedin Corp. No. 510-D36).

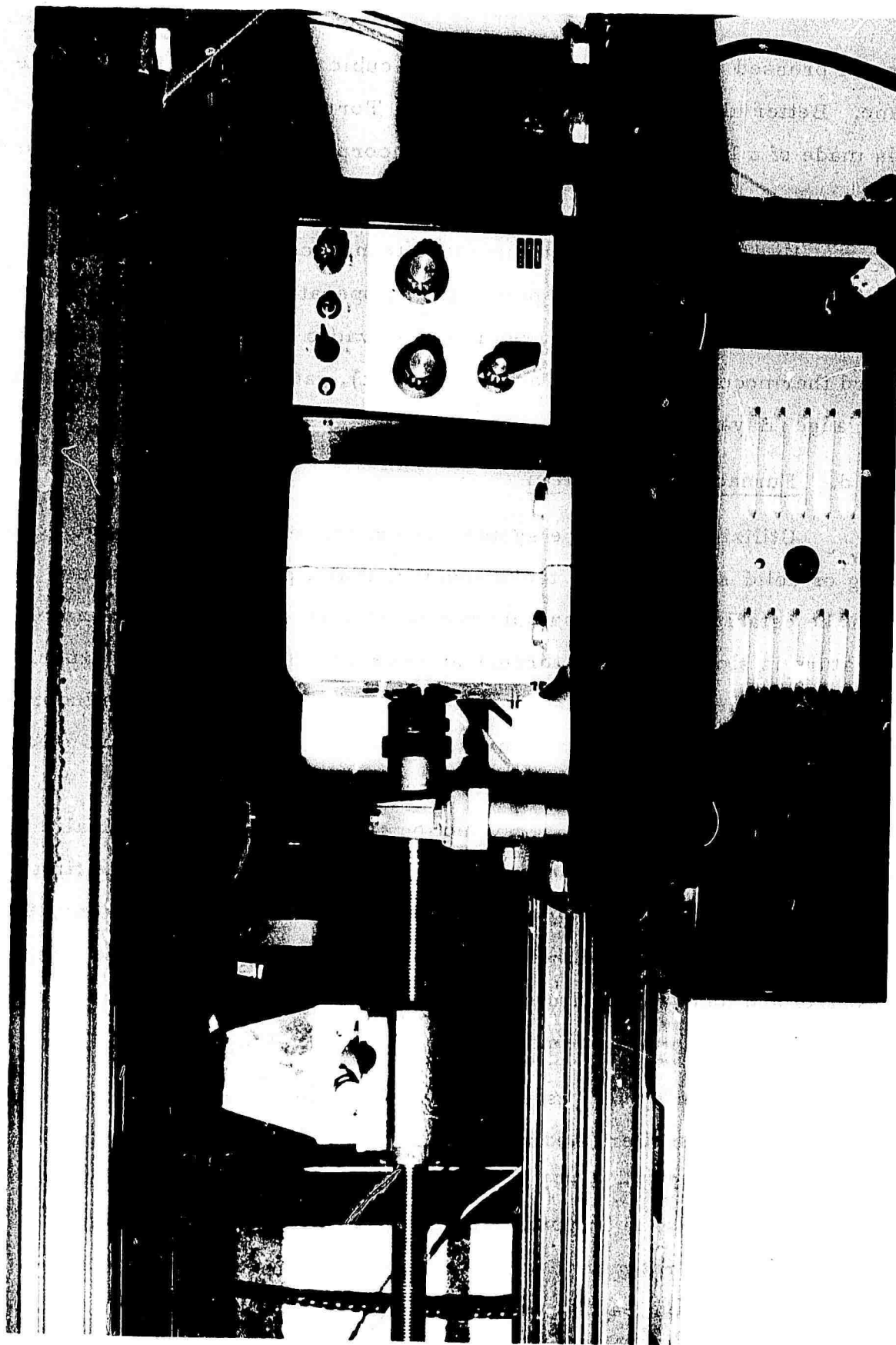


Figure 24. Drive system for furnace carriage, showing lead screw with coupling link to furnace (above), motor with speed reducer and electronic speed controller.

Rates of linear furnace movement of 1-50 mm per hour had initially been set as the design limits for any expected slow speed applications. The system components utilized have as the extreme limits the capability of driving the furnace 1/4-8400 mm per hour. Thus, the drive can also be used to remove the furnace from the tube, or to push it over it, at controlled speeds if samples have to be heated or cooled faster than the large heat capacity of the massive furnace would permit if the latter were kept stationary. If very rapid heating or cooling ("quenching") of a sample is desired, the furnace can be decoupled from the drive mechanism and moved manually. The furnace is mounted on a wheel base which runs on tracks long enough (6 feet) to allow its complete removal from the Mullite tube.

### 3. OPERATIONAL PERFORMANCE

Upon final assembly and installation of the total system, initial performance checks were conducted on each phase. Minor discrepancies which one normally expects in vacuum system check-out were rectified. The operational performance of the various electrical controls was checked out prior to establishing a uniform temperature gradient in the furnace.

Upon achieving satisfactory performance of each individual function of the system, several tests of the entire system, using representative cycles of high temperature-high vacuum programming, were performed. Controlled temperatures as high as  $1425^{\circ}\text{C}$  (limit of Mullite tube) with vacua reaching  $2 \times 10^{-5}$  Torr have been achieved and operational routines were established. High temperatures to the limit of the control system ( $1500^{\circ}\text{C}$ ) for an extended interval of time would necessitate the use of a more expensive alumina furnace tube in the place of the Mullite tube.

In the practical use of the furnace to date, several  $\text{RE}_2(\text{Co, Fe})_{17}$  alloy samples have been annealed in order to homogenize them, and a number of powder compacts have been successfully vacuum sintered in experiments with the liquid phase sintering of magnets. For this, a fixture was built which employs an alumina boat to support the samples and allows easy loading of the Mullite furnace tube through the brass flange end port.



As future applications require, different tube chamber inserts will be devised which have specialized sample and temperature monitoring fixtures and the necessary electrical connections to the sample.

## REFERENCES

1. A. E. Ray and G. I. Hoffer, Proc. 8th Rare Earth Research Conference, Reno, Nevada, April 1970, p. 524.
2. A. E. Ray, Proc. 7th Rare Earth Research Conference, Coronado, California, October 1968, p. 473.
3. K. Strnat, G. Hoffer, W. Ostertag, and J. C. Olsen, J. Appl. Phys. 37 (1966) 1252.
4. R. Lemaire, Cobalt, 33 (1966) 201.
5. K. H. J. Buschow and A. S. Van der Goot, J. Less-Common Metals, 14 (1968) 303.
6. F. Lihl, J. R. Ehold, H. R. Kirchmayr, and H. D. Wolf, Acta Physica Austriaca, 30 (1969) 164.
7. K. Strnat, W. Ostertag, N. J. Adams, and J. C. Olsen, Proc. 5th Rare Earth Research Conference, Ames, Iowa, August 1965, p. 57.

**BLANK PAGE**

DOCUMENT CONTROL DATA - R&D

(Security classification of title, body of abstract and indexing annotation must be entered when the overall report is classified)

1. ORIGINATING ACTIVITY (Corporate author) University of Dayton Research Institute Dayton, Ohio 45409		2a. REPORT SECURITY CLASSIFICATION Unclassified	
		2b. GROUP	
3. REPORT TITLE RESEARCH AND DEVELOPMENT OF RARE EARTH-TRANSITION METAL ALLOYS AS PERMANENT-MAGNET MATERIALS			
4. DESCRIPTIVE NOTES (Type of report and inclusive dates) Semiannual Interim Technical Report: 30 June 1970 - 31 December 1970			
5. AUTHOR(S) (Last name, first name, initial) Ray, Alden E. Strnat, Karl J.			
6. REPORT DATE March 1971		7a. TOTAL NO. OF PAGES 41	7b. NO. OF REFS 7
8a. CONTRACT OR GRANT NO. F33615-70-C-1625		9a. ORIGINATOR'S REPORT NUMBER(S) UDRI-TR-71-07	
b. PROJECT NO. 7371			
c. Task No. 737103		9b. OTHER REPORT NO(S) (Any other numbers that may be assigned this report) AFML-TR-71-53	
d.			
10. AVAILABILITY/LIMITATION NOTICES Distribution of this document is unlimited.			
11. SUPPLEMENTARY NOTES		12. SPONSORING MILITARY ACTIVITY Air Force Materials Laboratory Wright-Patterson AFB, Ohio 45433	
13. ABSTRACT Intermetallic phases with the formulas $R_2Co_{17}$ , $R_2Fe_{17}$ , and $R_2(Co_{1-x}Fe_x)_{17}$ are of potential interest as permanent magnets. Procedures for the preparation of these intermetallic phases are described. Descriptions are given of the design and operation of differential thermal analysis equipment and of a high temperature-high vacuum furnace for the metallurgical and magnetic evaluation of rare earth-transition metal intermetallic phases.			

14 KEY WORDS	LINK A		LINK B		LINK C	
	ROLE	WT	ROLE	WT	ROLE	WT
Magnetic Materials Permanent Magnets Rare Earth Alloys Intermetallic Compounds Preparation Methods Differential Thermal Analysis Equipment High Temperature-High Vacuum Furnace						

#### INSTRUCTIONS

1. **ORIGINATING ACTIVITY:** Enter the name and address of the contractor, subcontractor, grantee, Department of Defense activity or other organization (*corporate author*) issuing the report.

2a. **REPORT SECURITY CLASSIFICATION:** Enter the overall security classification of the report. Indicate whether "Restricted Data" is included. Marking is to be in accordance with appropriate security regulations.

2b. **GROUP:** Automatic downgrading is specified in DoD Directive 5200.10 and Armed Forces Industrial Manual. Enter the group number. Also, when applicable, show that optional markings have been used for Group 3 and Group 4 as authorized.

3. **REPORT TITLE:** Enter the complete report title in all capital letters. Titles in all cases should be unclassified. If a meaningful title cannot be selected without classification, show title classification in all capitals in parenthesis immediately following the title.

4. **DESCRIPTIVE NOTES:** If appropriate, enter the type of report, e.g., interim, progress, summary, annual, or final. Give the inclusive dates when a specific reporting period is covered.

5. **AUTHOR(S):** Enter the name(s) of author(s) as shown on or in the report. Enter last name, first name, middle initial. If military, show rank and branch of service. The name of the principal author is an absolute minimum requirement.

6. **REPORT DATE:** Enter the date of the report as day, month, year; or month, year. If more than one date appears on the report, use date of publication.

7a. **TOTAL NUMBER OF PAGES:** The total page count should follow normal pagination procedures, i.e., enter the number of pages containing information.

7b. **NUMBER OF REFERENCES:** Enter the total number of references cited in the report.

8a. **CONTRACT OR GRANT NUMBER:** If appropriate, enter the applicable number of the contract or grant under which the report was written.

8b, &c, & 8d. **PROJECT NUMBER:** Enter the appropriate military department identification, such as project number, subproject number, system numbers, task number, etc.

9a. **ORIGINATOR'S REPORT NUMBER(S):** Enter the official report number by which the document will be identified and controlled by the originating activity. This number must be unique to this report.

9b. **OTHER REPORT NUMBER(S):** If the report has been assigned any other report numbers (*either by the originator or by the sponsor*), also enter this number(s).

10. **AVAILABILITY/LIMITATION NOTICES:** Enter any limitations on further dissemination of the report, other than those

imposed by security classification, using standard statements such as:

- (1) "Qualified requesters may obtain copies of this report from DDC."
- (2) "Foreign announcement and dissemination of this report by DDC is not authorized."
- (3) "U. S. Government agencies may obtain copies of this report directly from DDC. Other qualified DDC users shall request through \_\_\_\_\_."
- (4) "U. S. military agencies may obtain copies of this report directly from DDC. Other qualified users shall request through \_\_\_\_\_."
- (5) "All distribution of this report is controlled. Qualified DDC users shall request through \_\_\_\_\_."

If the report has been furnished to the Office of Technical Services, Department of Commerce, for sale to the public, indicate this fact and enter the price, if known.

11. **SUPPLEMENTARY NOTES:** Use for additional explanatory notes.

12. **SPONSORING MILITARY ACTIVITY:** Enter the name of the departmental project office or laboratory sponsoring (*paying for*) the research and development. Include address.

13. **ABSTRACT:** Enter an abstract giving a brief and factual summary of the document indicative of the report, even though it may also appear elsewhere in the body of the technical report. If additional space is required, a continuation sheet shall be attached.

It is highly desirable that the abstract of classified reports be unclassified. Each paragraph of the abstract shall end with an indication of the military security classification of the information in the paragraph, represented as (TS), (S), (C), or (U).

There is no limitation on the length of the abstract. However, the suggested length is from 150 to 225 words.

14. **KEY WORDS:** Key words are technically meaningful terms or short phrases that characterize a report and may be used as index entries for cataloging the report. Key words must be selected so that no security classification is required. Identifiers, such as equipment model designation, trade name, military project code name, geographic location, may be used as key words but will be followed by an indication of technical context. The assignment of links, rules, and weights is optional.